Placement and Routing for Cross-Referencing Digital Microfluidic Biochips

Zigang Xiao and Evageline F. Y. Young

***Abstract*—Computer-aided Design (CAD) problems of Digital Microfluidic Biochips (DMFB) are receiving much attention, and most of the previous works focus on direct-addressing biochips. In this paper, we solve the placement and droplet routing problem in *cross-referencing biochips*. In these biochips, the electrodes are addressed in a row-column manner, which may cause *electrode interference* that prevents simultaneous movements of multiple droplets. We propose a routing algorithm that solves the droplet routing problem directly. A two-coloring graph-theoretic method is used in our router to detect and prevent the electrode interference. In addition, we propose an Integer Linear Programming (ILP) based method to solve the placement problem. Our method considers the characteristics of cross-referencing biochips and is aware of droplet routing. Real-life benchmarks are used to evaluate the proposed methods. Compared with previous works, our router improves on average 4% in routing time and 58% in runtime. It can route all the benchmarks within the time limits, while the latest work fails in some cases. Moreover, experimental results show that by running our router on the placement result generated by our method and those generated by the latest work, an average improvement of 11% 29%, 54% and 46% in the maximum routing time, average routing time, stalling steps and cell usage can be achieved.**

***Index Terms*—microfluidics, biochip, cross-referencing, placement, routing, droplet.**

I. Introduction

MICROFLUIDIC-BASED biochips have received much attention today [1]. It shows great advantages in medical, pharmaceutical and environmental monitoring applications [2]. Instances include immunoassays for point-of-care medical diagnostics, DNA sequencing and detection of airborne particulate matter [2], [3], [4], [5], [6], [7], [8], [9]. In contrast to conventional expensive and tedious laboratory procedures, advantages of miniaturized biochips include higher sensitivity, lower cost due to smaller sample and reagent volumes, higher levels of system integration, less human resource and less likelihood of human error [10]. As a result, markets are opening up for such kind of devices. For example, the worldwide market for *in-vitro* diagnostics in 2007 was estimated at $38 billion [11]. The remarkable market indicates a prospective future of biochips.

Traditional biochips utilize continuous-flow microfluidic technologies. In continuous-flow systems, flow of liquid is piped through micro-fabricated channels. Simple and well-defined applications are made available in these systems. However, they are not suitable for highly complicate fluid manipulation because of the inherent complicated nature of continuous liquid flow. The design and analysis of these systems are barely tractable even for a moderate complex application. In addition, the systems have to be custom-made according to specific applications, because of the tight coupling of the system implementation and the functionality.

Digital microfluidic technology is utilized in second generation biochips. In these systems, nano-level biochemical material can be transported and processed in the form of tiny discrete 'droplets'. Precise control of nanoliter droplets that contain biochemical reagents, samples and buffers are made available in these devices. As a result, basic operation units such as mixing, detection and diluting can be built. Consequently, various kinds of biochemical reaction can be modeled and performed on this platform. Hence, biochips can be viewed as miniaturized laboratories, i.e., 'lab-on-a-chip'. The droplets can be imported onto the chip via *dispensing* ports, and can be exported via *reservoir* ports. There is a parallel pair of top and bottom plates of electrodes in the basic design of such systems. The bottom plate contains a patterned array, in which each electrode can be addressed independently, while the top plate is filled with ground electrode. A droplet can be moved to one of its four neighboring cells by applying a control voltage over the target cell and at the same time deactivating the electrode at the droplet's current position. Interfacial tension gradients will then be generated by the electronic manipulation, and the droplet will be dragged to the activated electrode. Consequently, the droplets can be moved to any free cells on the array. Detectors such as photodiodes and LEDs can also be integrated into the biochips to perform optical monitoring tasks. Fig. 1(a) gives a schematic diagram of a digital microfluidic biochip (DMFB) [12]. In contrast to previous continuous-flow biochip systems, DMFBs offers an important property, i.e., *dynamic reconfigurability* [13], because fluidic operations can be performed anywhere on the array. Hence, microfluidic modules can be viewed as 'virtual devices', with the corresponding droplet being routed by applying a series of adjacent electrodes. For instance, the mixing operation is accomplished by moving two droplets to the same location first, and then driving them together around some pivot point. Also, the operations can be reconfigured into different sizes [10]. The reconfigurability of DMFBs will be further discussed in Section II-B.

With its flexible design, many tasks can be performed in DMFBs without using expensive equipment and human

Z. Xiao is with the Department of Electrical and Computer Engineering, University of Illinois at Urbana-Champaign, Champaign, IL 61820, USA (email: zxiao2@illinois.edu).

E. F. Y. Young is with the Department of Computer Science and Engineering, Chinese University of Hong Kong, Hong Kong, China (e-mail: fyyoung@cse.cuhk.edu.hk).

resource. However, there is still not much existing design automation techniques for DMFBs. Thus, computer-aided design support is strongly needed for DMFBs as in traditional VLSI design. In paper [14], a novel top-down design methodology for DMFBs is proposed. In this paper, the design of biochips is divided into *architectural-level* and *geometry-level* synthesis. The behavioral model for a biochemical assay is first acquired from the laboratory protocol and modeled as a sequencing graph. Then, architectural-level synthesis follows to generate the macroscopic structure of the biochip. *Task scheduling* and *resource binding* are then performed to schedule assay functions and bind them to existing resources so as to minimize assay completion time. Next, geometry-level synthesis that includes the module *placement* and *droplet routing* is performed to generate the detailed layout of the biochip. Analogous to traditional VLSI design, this methodology decouples the complex design flow into several tractable subproblems. Designers can thus solve the whole problem in several manageable pieces. The overall synthesis flow is given in Fig. 2.

Another important design consideration of biochips is the electrode manipulation method. It refers to the manner that the electrodes are controlled and activated by input pins. In a DMFB, the movements of droplets are controlled by the electro-hydrodynamic forces generated by the electrodes. Early designs of biochips used direct-addressing manipulation scheme, in which every electrode is associated with an input pin. Each cell can thus be addressed independently to bring about the droplets' movement. Although this scheme is straightforward and simple, it is not suitable for large array applications because the need for a large number of control pins will increase the production cost significantly. Pin-constrained addressing schemes are proposed to scale down the number of control pins. These schemes map the electrodes to a smaller number of control pins. In other words, each pin controls more than one electrodes. Droplet-trace-based array partitioning method [15] and broadcast-addressing method [16] are two commonly seen methods. However, both of them lead to mappings of pins that are inevitably specific to some target application. A more promising design is *cross-referencing* electrode manipulation scheme, which addresses the electrodes in a row-column manner. Biochips that use this scheme are called *cross-referencing* biochips, in which high and low (or low and high) voltages are applied to a row electrode x and a column electrode y respectively so as to *activate* the cell at the intersection point (x, y). Fig. 1(b) gives an example of a cross-referencing biochip [17].

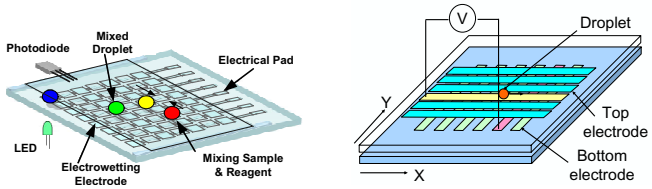

(a) (b)

Fig. 1. (a) Schematic view of a DMFB. (b) A Cross-referencing biochip.

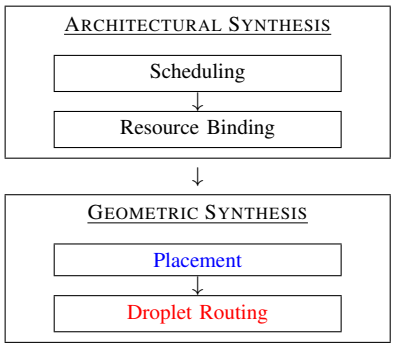

Fig. 2. Synthesis flow of DMFB.

However, because the control of the activation of a cell is in a row-column manner, *extra cells* may be activated when several droplets are moving together. Thus the droplets may be affected unintentionally. This unwanted effect is referred as *electrode interference*, and *electrode constraints* should be imposed to avoid such erroneous cases during droplet routing. Cross-referencing imposes tighter constraints to simultaneous manipulation of droplets' movements than direct-addressing. Nevertheless, one can maximize the parallelism by carefully arranging voltages. This will be further discussed in the following sections.

In this paper, we present automated design methods for the placement and droplet routing problem in cross-referencing digital microfluidic biochips. Our placement method considers the properties of cross-referencing biochips and generates a routing input that is more suitable for cross-referencing biochip routers. In our router, a graph two-coloring method is used to address the electrode interference issue. It is shown that by combining both methods, high-throughput routing solution with high defect-tolerance for cross-referencing biochips can be achieved. The 'GEOMETRIC SYNTHESIS' box in Fig. 2 shows the entire flow of our algorithms.

The rest of this paper is organized as follows. Section II gives more details about the cross-referencing biochips and the electrode interference issue, as well as the placement and droplet routing problem on it. In Section III, we discuss the related prior works on both problems and present our contributions. Section IV and Section V describe our methods for the droplet routing problem and the placement problem. Note that in our approach to solve the placement problem, we will consider the properties of cross-referencing biochips and some details about droplet routing. Hence, in order to better explain our method, the routing sub-problem and our proposed router will be introduced in Section IV first. The placement problem and our approach will be introduced in Section V. Experimental results will be given in Section VI. Finally, conclusions will be drawn in Section VII.

II. PLACEMENT AND ROUTING IN CROSS-REFERENCING DIGITAL MICROFLUIDIC BIOCHIPS

In this section, we will give more detail about cross-referencing biochips and the unique electrode interference issue. Placement and routing problem in this kind of device will also be discussed.

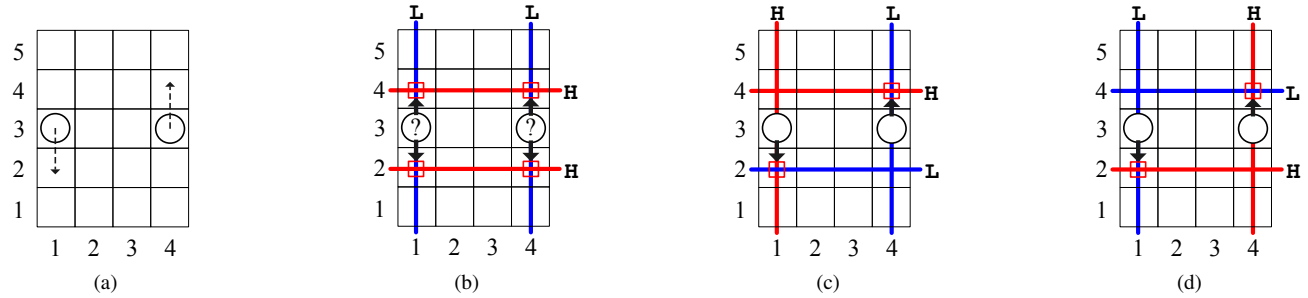

Fig. 3. (a) The two droplets are moving from current cell to the arrow-pointed cell. (b) Electrode interference happens. Droplets' movements are intervened. (c) Solution: apply voltage appropriately. (d) An alternative solution.

A. Electrode Interference

In cross-referencing biochips, the control of the activation of a cell is in a row-column manner. *Extra cells* may be activated when more than one droplets are manipulated at the same time. Thus, some droplets may be affected by the *extra-activated cells* unintentionally. Hence, cross-referencing electrode manipulation scheme imposes tighter constraints to simultaneous manipulation of droplets' movements than direct-addressing scheme. An example is given in Fig. 3. Suppose the left droplet needs to be moved from (1,3) to (1,2), while another droplet needs to be from (4,3) to (4,4). We assign high voltage to row 2 and 4, as in Fig. 3(b), while assigning low voltage to column 1 and 4, so as to activate both cells (1,2) and (4,4). However, cells (1,4) and (4,2) will also be activated, and they are called *extra-activated*. Hence, the droplets may not be moved as planned. If appropriate voltage assignment can be performed as in Fig. 3(c), correct movements can be guaranteed. Fig. 3(d) is an alternative solution by flipping all the electrodes in Fig. 3(c) to its opposite value. For rows and columns that are not marked as 'H' or 'L', ground voltage is assigned and no cells will be activated along those rows and columns. Note that those extra-activated cells do not necessarily imply electrode interference. If no droplet is around the extra-activated cell, no electrode interference will ever happen. The main challenge of routing droplet in cross-referencing DMFBs is to avoid electrode interference. In this sense, cross-referencing DMFBs have much tighter constraint than direct-addressing ones, which means the throughput may be severely decreased. However, as the example suggests, with the help of a well-designed router, cross-referencing biochips can still achieve high-throughput that is as good as that in direct-addressing biochips.

B. Placement in DMFB

Given scheduling and resource binding results generated from architectural-level synthesis, the placement problem involves placing the microfluidic modules and optimizing some design metrics while satisfying various constraints. The objective is to place all the modules in the biochip and maximize the routability for later routing problems. Meanwhile, we want to maintain high fault-tolerance. We will discuss fault-tolerance of DMFBs later. Note that the placement problem of DMFBs is different from the traditional placement problem in electronic design [18] because of the reconfigurability. Since the biochips are reconfigurable, the modules are 'virtual devices' that can be placed anywhere in the biochips as long as they do not overlap with each other at a specific time. However, the modules cannot be placed adjacent to the dispensing port; otherwise, it will block the importing of droplets.

Placement is a critical step before the droplet routing. It will directly affect the routability and routing quality. One of the bad consequences is that the placement result is totally unroutable as shown in Fig. 4(a). Due to the dynamic reconfigurability of biochips, this can be solved by moving Block 1 down to the bottom so as to create a path for the droplet. In another case, the placement solution may have a poor quality in terms of throughput. As in Fig. 4(b), the modules may be placed in an over-congested way that one droplet may have to wait for another droplet to pass by, which makes the routing very sequential. Another example is shown in Fig. 5. Suppose the router will generate routes that use a shortest path for both placements. Apparently, the overall routing distance of the droplets in placement solution (a) is larger than that in placement solution (b). There are at least two reasons to minimize the overall routing distance. Firstly, the shorter routing distance a droplet has, the more flexibility it will gain to finish the route within timing limit, which also increases routability. Secondly, this is beneficial to fault-tolerance since fewer cells are used. In conclusion, placement stage should be carefully implemented in order to provide better input configuration for the later routing problem.

In this paper, we propose a comprehensive method that solves the placement problem by considering the properties of cross-referencing DMFBs. The motivation is that the properties observed from cross-referencing are easy to model and naturally fitted into ILP objective function. Moreover, feasible result can be obtained and improved in an iterative manner when using ILP.

C. Droplet Routing in DMFB

After the placement phase, routing will be done. The output of placement consists of locations of operations, i.e., modules. Before an operation can take place, the droplets have to be transported to the corresponding locations. Hence, the objective of droplet routing is to find valid routes for all the droplets without causing unexpected mixture, and the number of cells used should be minimized for better fault-tolerance. Note that between two successive operations, a

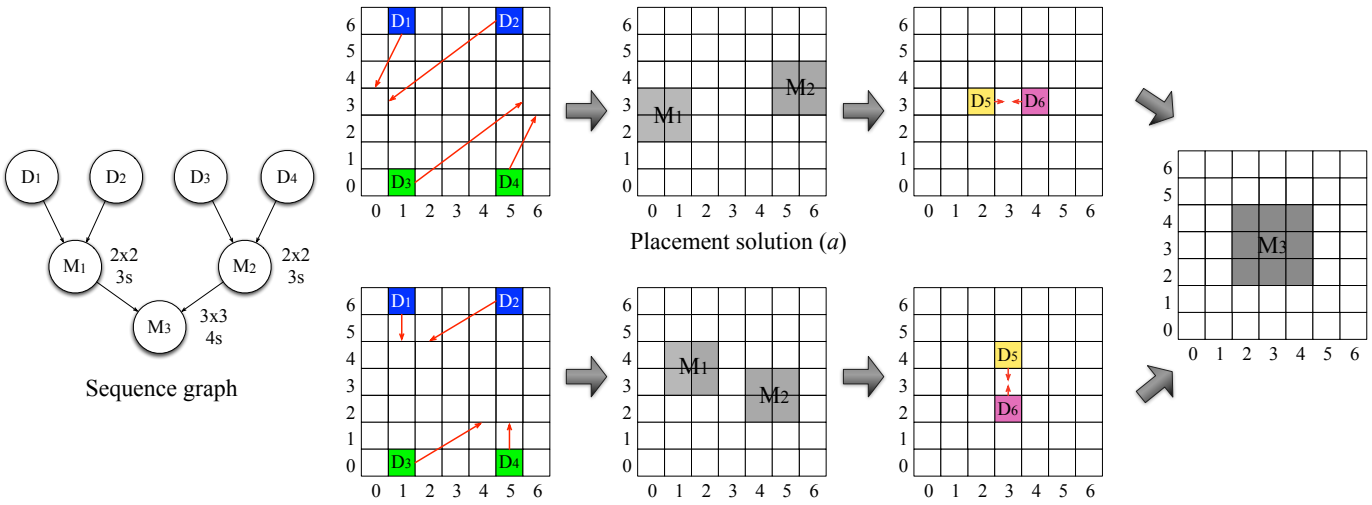

Fig. 5. Example of different placement solutions. The figure on the left is the sequence graph generated from the input. M_1, M_2 and M_3 are mixing modules. D_5 and D_6 are the output droplet from M_1 and M_2, respectively.

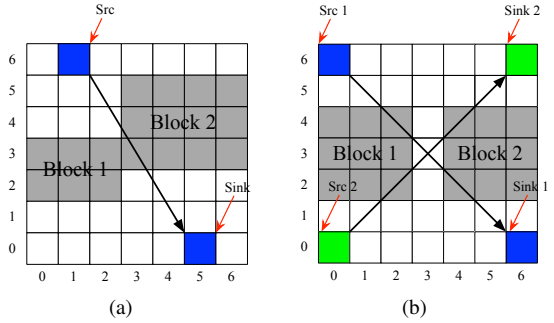

Fig. 4. (a) Two modules block the path of the net. This placement is unroutable. (b) Although the path is not blocked. The two droplet has to coordinate which one should go first. Otherwise, they will form a deadlock in the critical path.

certain amount of time interval is assumed be reserved for routing the droplets. This forms the *timing constraint* of the droplet routing problem [12]. Although this time interval is relatively small comparing to the duration of each sub-operation (e.g., 0.2s vs. 2s), it is desirable to be minimized to prevent spoilage and ensure the correctness of subsequent operations. During droplet routing, at least one cell should be kept between droplets to prevent unintended mixing, except when droplets are to be mixed intentionally. Hence, *static fluidic constraint* and *dynamic fluidic constraint* are introduced between two droplets [12] to restrict the locations of droplets. Furthermore, recall that high and low (or low and high) voltage needs to be assigned to the row and column electrodes without causing electrode interference. This can be modeled as *electrode constraint* to ensure the correctness of droplet movements. Finally, the number of cells used by droplets during routing is preferred to be minimized to achieve better fault tolerance and robustness. As discussed in paper [**?**], minimization of the droplet routes lead to the minimization of the total number of cells used during routing. More spare cells are freed for fault-tolerance [14]. Finally, after the solution (routes of droplets) is found, it can be stored into the DMFBs to perform pre-programmed biochemical operations. Hence droplet routing is a fundamental design step and crucial to the reconfigurability of DMFBs.

Note that the blocks in droplet routing are different from the blocks in traditional routing. In fact, they are *on-going operations*. Due to the reconfigurability of DMFB, these operations can be done anywhere on the biochip. In order not to violate the fluidic constraint [12], a *guarding ring* is imposed around a module with on-going operation. During routing, if the droplet inside a module is pulled outside unintentionally, the correctness of the whole bioassay will be ruined. Hence, it is very important to ensure the droplet staying inside a module when the operation is still in progress. However, as introduced in Section I, there may be extra-activated cells on the biochip during droplet routing. They are allowed to exist if and only if no electrode interference will be caused. Nevertheless, previous works on routing did not consider this potential problem. In this paper, we forbid the cells in the guarding ring to be activated in order to prevent the droplet inside from being pulled out. The cells inside the guarding ring are allowed to be activated because the droplet inside will not be pulled out in any way. An example is illustrated in Fig. 6.

III. Previous Works and Our Contribution

A. Previous Works On Placement

There are several papers trying to solve the placement problem, but as long as we know, there is no previous work on placement for cross-referencing biochips. Su *et al.* presented a simulated annealing-based algorithm in [19]. They try to take the fault tolerance issue into consideration by computing a ratio between the number of fault-free cells and the total number of cells. A unified synthesis algorithm is proposed by Su *et al.* in [20], in which placement is one of the steps. In their paper, a parallel recombinative simulated annealing that combines scheduling, resource binding and placement together is proposed. Later, they even include routing into the annealing process [21]. They claimed that the synthesis and placement of DMFBs is very similar to the operation of dynamically reconfigurable FPGAs (DRFPGAs) [22]. Yuh *et al.* proposed

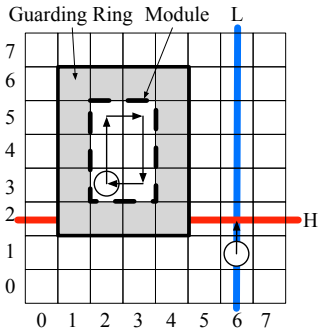

Fig. 6. A droplet is inside a mixing module and another droplet is moving upwards. The gray region denotes the guarding ring of the module. Note that low voltage cannot be assigned to column 1∼4 in this case because otherwise, the cells in the guarding ring will be extra-activated.

several representations in simulated annealing-based methods for the floorplanning problem, including *3D-subTCG* [23] and *T-tree* [24]. They adopt the T-tree formulation to solve the placement problem in biochips [25]. This method is derived from the well-known 2-D placement method for reconfigurable devices. Defect cells are also modeled and considered in their work.

B. Previous Works On Routing

Existing methods of solving the cross-referencing droplet routing problem can be classified into two categories. The first category is to get a direct-addressing solution first, and then convert the solution to satisfy the electrode constraint in cross-referencing biochips. Griffith *et al*. tackles the problem using a graph coloring approach [26]. The problem is treated as a direct-addressing one and is solved first using a direct addressing method introduced in one of his previous works [27]. The solution is then converted to a cross-referencing result by coloring an interference graph. Su *et al*. proposed a two stage process to solve the direct addressing droplet routing problem [12], the result is then modified to adapt to cross-referencing DMFBs by Xu *et al*. using a *clique partitioning* approach [28]. Since there are many existing methods for direct-addressing droplet routing, it is reasonable to adapt them for cross-referencing DMFB. Nonetheless, this kind of approach may be myopic since it loses the global view of the problem. The second category is to solve the problem directly, which is not limited by the direct-addressing result right from the beginning. Yuh *et al*. proposed an integer linear programming (ILP) based method to solve the problem [17]. They claim that it is the first method that directly solves the problem, not relying on a direct-addressing result. The movement of droplets at each time step is determined by solving an ILP. A 'droplet movement cost' is used to evaluate congestion when solving the ILP. This method works directly on cross-referencing biochips, and hence better result can be obtained. However, their approach cannot guarantee to finish all the routings within a given timing constraint and thus may eventually result in failure of the whole bio-application.

C. Our Contributions

In this paper, a placement method is proposed to solve the placement problem in cross-referencing biochip. The properties of cross-referencing biochips are utilized in the proposed method in order to generate a good placement result that is more suitable for routing of biochips. Meanwhile, we propose a method called CrossRouter that directly solves the droplet routing problem on cross-referencing biochips. Our goal is to simultaneously move a group of droplets as much as possible to maximize the parallelism and to minimize the total transportation time, as well as minimizing the total number of cells used during the routing process. The major contributions of our work include:

- We propose an ILP-based method that solves the placement problem for cross-referencing biochips. Our method considers the properties of cross-referencing and is droplet-routing-aware. The effectiveness of our method is verified by running the proposed router on the placement results generated by our method and those by previous works respectively. Experimental results suggest that our method can generate placements that are more suitable for cross-referencing biochip routers. To tackle the complexity of the ILP, a partitioning method is included. A maze routing is utilized in our pin assignment stage to eliminate unroutable solutions. Routability can be improved significantly with these extensions.
- We design a router that directly solves the droplet routing problem in cross-referencing biochips. An elegant two-coloring approach is used in our router to handle the stringent electrode constraints. Experimental results show that the proposed router can achieve shorter routing time on average and can satisfy the timing constraints in all problems. Moreover, the number of cells used in the solution generated by our router is close to that in [29], although [29] is working on direct-addressing biochips that do not have those stringent electrode constraints. The extra-activated cells on the guarding ring of a module (see Section II-C) are handled in our router to avoid unwanted effects. A new rip-up and re-route process is designed for the router in which a probability-based scheme is used to allow non-deterministic ripping, which can break infinite looping effectively.

IV. Our Router for Cross-Referencing Biochip

A. Droplet Routing Problem

In this problem, all the droplets on a biochip must be routed to their destinations subject to some constraints. A cross-referencing DMFB can be viewed as a 2D array with W rows and H columns. Each cell on the biochip can be referred to as (X, Y). There are D droplets and B blockages on the biochip. The fluidic ports on the boundary of a module, dispensers and waste reservoir are called *pins*. They are used to denote the source and destination of a droplet in its route. For example, if a droplet d_i is to be routed from module M_1 to module M_2, we need to know the source pin location that is around M_1 and the sink pin location that is around M_2 so as to compute a route for d_i. Droplet route between the pins of different

modules are modeled as *nets* [12]. Each droplet is either in a *2-pin net* or a *3-pin net*. A 2-pin net refers to a route that a single droplet needs to be routed from its source to sink, while a 3-pin net contains two droplets that start from different sources and reach at the same sink. There are totally N nets on the biochip. Given a droplet d_i (net i), we denote the start location and the end location of d_i as *source* s_i and *sink* t_i. As we mentioned, there is a *waste reservoir* on the biochip. When a droplet reaches such locations, it will be removed from the biochip at next time step. Finally, a time limit T is given, which is an upper bound on the total amount of time used to route all the nets. The output of the problem will be a *schedule of voltage assignment* at each time step. This is different from the droplet routing problem in a direct-addressing biochip. The schedule of voltage assignment includes a correct manipulation sequence of electrodes, and it implies the movements of the droplets during the whole routing process. Note that we will target at minimizing the arrival times of the droplets at their destinations besides satisfying the timing constraint, since the time for droplet routing is part of the incoming bio-operation time [12]. Meanwhile, the number of cells used needs to be minimized, since it directly relates to the fault tolerance of the biochip. Considering all the constraints mentioned previously, the problem can be formulated as: Given chip specification, assay description and placement results as input, route all the nets within time limit without violating fluidic and electrode constraints while minimizing the cells used for routing.

B. Overview of Our Router

In this section, we will detail a droplet routing method that named as CrossRouter. In principle, our method first gets a reasonable routing order, and then each net is processed according to this order, while considering the nets that have already been processed. Rip-up and re-route will be performed if a net is unsuccessfully routed. The process continues until all the nets are routed. The solution obtained by our method contains a valid voltage assignment sequence in different time steps, which ensures that each droplet reaches its destination cell within time T without causing any violation. If the time limit for rip-up and re-route is exceeded, the routing process will be stopped, and failure will be reported to the previous synthesis stage, i.e., placement, etc. Tasks should then be re-assigned or module should be replaced in order to avoid over-congested routing configuration.

When routing a net, there are two stages. The first stage is called *propagation*. Our algorithm tries to find a valid shortest path for a net in this stage. The propagation starts from the source of a net, and ends when it reaches the destination. Fluidic and electrode constraint check will be performed in each propagation step. A 3D bitmap technique is used to enable quick detection of fluidic constraint violation, while an incremental two-coloring method is used during electrode constraint check to seek if there exists a feasible voltage assignment to implement the current set of droplet movements. A penalty count for each previously processed net will be incremented by one if it causes violation when routing the current net. These counts are used in the rip-up and re-route step to select the net to be ripped up. The second stage is the *backtracking* stage. After a valid path is found at the propagation stage, voltage assignment is *incrementally* performed based on the routing result. An overview of our algorithm is given in Algorithm 1.

Algorithm 1: CROSSROUTER

Input: Chip configuration and net information.
Output: Voltage assignment for each time step.

```
1  begin
2      queue ← COMPUTENETORDER(N);
3      while queue is not empty do
4          net ← pop out head element of queue ;
5          while net is not routed successfully do
6              result ← PROPAGATION(net);
7              if result = Success then
8                  BACKTRACK(net);
9              else if net is the first net being routed then
10                 Report failure and exit;
11             else RIPUPREROUTE(net);
12         end
13     end
14 end
```

C. Net Order Computation

The net order is computed before the routing actually begins. We first give a formal definition of the *bounding box of a net*:

Definition 1 (Bounding Box)**.** *A bounding box of a net is defined as the rectangular area of the maximum extent of the source pin and sink pin.*

Intuitively, it is the rectangle defined by $min(x)$, $max(x)$, $min(y)$ and $max(y)$ where x and y are the x-coordinate and y-coordinate of the pins in a net.

The net order is computed according to the following conditions in descending precedence: 1) If a net i's source point is inside the bounding box of another net j, i should be routed before j. Otherwise, it may be blocked by j during its routing. 2) Nets with a larger Manhattan distance from the source point to the sink point should be routed earlier, because all the nets have the same timing limits, but these nets have a longer distance to move.

D. Propagation Stage

In this stage, for a given net d_i, the router tries to find a route $\{d_i^0, d_i^1, \ldots, d_i^T\}$ from its source to its sink without violating any constraint or causing any interference. In contrast to traditional routing, the route of a net here is the temporal positions of a droplet within the timing constraint, and is subject to the control of the electrodes.

Here we present how the possible routes of a net are explored in CrossRouter. During the propagation, a droplet d_i may reach a cell Q=(Q_x,Q_y) at time $t-1$ and move to one of its adjacent cells P at time t. The pair (Q,t), called a

droplet movement status, denotes the position of the droplet at time t. (Q,$t-1$) is called the *parent* of (P,t) and is denoted by (Q,$t-1$) = *parent*((P,t)). There are five possible movements for the droplet at time t. They are *LEFT, RIGHT, UP, DOWN* and *STALL*. For example, when droplet is at (3,6) at t=3, then at t=4, it can be moved to either one of (2,6), (4,6), (3,7), (3,5), or stall at the same position (3,6). By following the parents of a status (P,t) all the way back, one can always trace out the route by which d_i is transported to P. Starting from a source point, a set of statuses is explored iteratively until the sink point is discovered. In order to find a desired path earlier, a *weight* is assigned to each status. It is calculated as follows:

$$weight(P,t) = t + MD(P,s_i) + Len(P,t) + U(P)$$

where $MD(A,B)$ is the Manhattan distance from A to B, $U(P) = N - \#used$, N is number of nets and $\#used$ is the number of nets that used this cell before, and $Len(P,t)$ is the length of the current path from the source point to P at t. In this weight function, we want to minimize t so as to satisfy timing limit. $MD(P,s_i)$ is a standard term in similar maze routing weight function that is used to control the path length. However, detour of cycles may exist in the routing path. $Len(P,t)$ measures the real path length and assigns a higher weight to this kind of path. Finally, $U(P)$ is used to minimize the cells used.

A sorted list of such statuses is maintained to record the routes that have been explored. In each iteration, the status (P,t) with the smallest weight is chosen. If the sink point is reached at time t, fluidic and electrode check should be performed from time $t+1$ to T so as to ensure that this droplet will not block any processed net. Otherwise, new statuses due to propagation from P at time $t+1$ will be added into the list, subject to the constraints that we will discuss in the next section. If the sink point is not reached and the list becomes empty, the routing of this net is failed. Rip-up and re-route will be performed. The fluidic and electrode constraint can be checked as follows:

1) Fluidic Constraint Check: Fluidic constraint check should be performed in order to prevent unexpected mixing of droplets during their transportation. To be more formal, let $d_i^t = (x_i^t, y_i^t)$ denote the location of droplet i at time t. Note that $s_i = d_i^0$ and $t_i = d_i^T$. The static and dynamic fluidic constraints can be stated as:

$$\begin{array}{llll} |x_i^t - x_j^t| \geqslant 2 & \textbf{or} & |y_i^t - y_j^t| \geqslant 2 & \textbf{and} \\ |x_i^t - x_j^{t-1}| \geqslant 2 & \textbf{or} & |y_i^t - y_j^{t-1}| \geqslant 2 & \end{array}$$

Furthermore, as the routing can be viewed as a 3D routing, in our implementation, we use a 3D bitmap to speed up the check.

2) Electrode Constraint Check: Electrode constraint check is a crucial part in CrossRouter. We can show that, when there are only two moving droplets, there will always be a valid voltage assignment to move them correctly without causing any electrode interference. An example is illustrated in Fig. 3. However, conflict may happen among three simultaneously moving droplets, because the conditions to activate and de-activate some cells may be contradictory. In this paper, we introduce a succinct graph coloring based method to determine whether the simultaneous movements of a set of droplets are feasible or not, i.e., whether a valid voltage assignment exists to implement the movements of several droplets at the same time. In contrast to the method proposed by Griffith [27], our approach do not attempt to find the chromatic number for a graph, which is NP-hard in general, but rather determines whether a movement is implementable. We will make use of a special type of *constraint graph* to perform this check.

A constraint graph $G = (V,E)$ in our context is an undirected graph that consists of two types of edges. The first kind is called *DIFF* edge, which means that the vertices at its two ends must have different colors, and the second kind is called *SAME* edge, which means that the adjacent vertices should have the same color. A two-coloring in this constraint graph is an assignment of two colors to the vertices such that the vertices sharing a *DIFF* edge have different colors, while the vertices sharing a *SAME* edge have the same color. As discussed before, we can apply a high, low or ground voltage to a row or column and a cell will be activated when its intersecting row and column are assigned high and low (or low and high) respectively. In our electrode constraint check, we will have a vertex representing a row or a column in the constraint graph if this row or column must be set to a high or a low voltage in order to activate some cells. For those rows or columns which are not represented by a vertex in the graph, they are supposed to be set to the ground voltage and thus will not cause any electrode interference. Clearly, it is a polynomial time reduction from the instance of the voltage assignment constraint to the instance of constraint graph, which is a one-to-one correspondence. This concept is important allowing us to be able to check the electrode constraint efficiently using two-coloring.

At time t, a constraint graph G_t will be constructed according to the droplets' movements. We will insert vertices and edges into G_t in such a way that *there is a one-to-one correspondence between two-coloring of the graph and feasible voltage assignment on the biochip.* We will explain below how G_t will be constructed. We use $C(X)$ to denote a vertex in G_t that represents a column X and use $R(Y)$ to denote a vertex representing row Y. During the transition of a droplet from one cell Q to one of its adjacent cells P, only P is allowed to be activated in the droplet's *4 × 3 bounding box (BB)*, which is formed by the neighboring cells of P and Q. Note that the outer row/column perpendicular to the moving direction of the droplets is also forbidden, since its activation may cause unexpected movement of the droplet after it settles in P at time $t+1$. However, if the droplet is stalling, all the cells in the droplet's 3×3 *BB* cannot be activated, while the droplet's current location Q can be activated or not.

According to the rules above, the constraints can be modeled by adding different types of edges into the graph. First of all, vertices $C(X)$ and $R(Y)$ will be added into G_t if and only if there is a droplet moving to the cell at (X,Y) at time t. We consider the move and stall action separately as follows:

- If a droplet d_i is moving from Q to $P = (P_x, P_y)$, add a *DIFF* edge between $C(P_x)$ and $R(P_y)$. This is to activate the cell at P. For any neighboring cells (X,Y) of P and Q, if both $R(X)$ and $C(Y)$ exists in G_t (due to d_i or

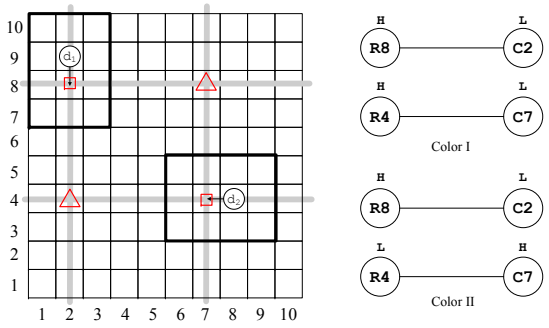

(a) Chip scenario and constraint graph considering d_1 and d_2 only. Two asymmetric two-coloring solution are showed while color I activates more cells (marked with 'Δ')

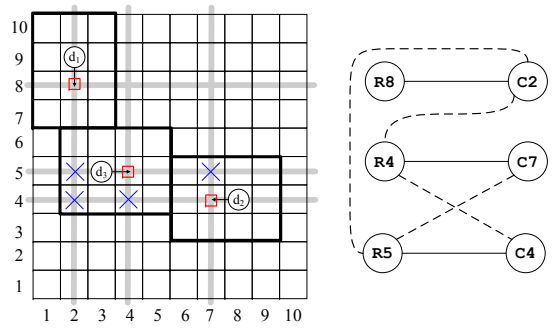

(b) Chip scenario and constraint graph considering d_1, d_2 and d_3 simultaneously.

Fig. 7. Example of checking electrode interference with constraint graph

other droplets), add a *SAME* edge between $C(X)$ and $R(Y)$. This is to make sure that the neighboring cells are not activated.

- If a droplet d_i is stalling at its current position P, we consider its neighboring cells (X, Y). If both $R(X)$ and $C(Y)$ exists in G_t (due to other droplets), add a *SAME* edge between $C(X)$ and $R(Y)$. This is to make sure that the neighboring cells are not activated.

After constructing G_t, we can determine whether G_t has a two-coloring, which can be done efficiently. We can easily see that the existence of a two-coloring in G_t is equivalent to having a feasible voltage assignment to the rows and columns such that all droplets' movements can be achieved simultaneously. We illustrate the idea by giving a concrete example in Fig. 7 to demonstrate the construction and coloring of the constraint graph.

The shaded bars are the rows and columns at which we need to apply high or low voltages. Small rectangles are the cell to be activated. The solid lines in the graphs on the right represent *DIFF* edges while the dotted lines represent *SAME* edges.

Fig. 7(a) shows an example that the router is routing d_2 at some time step while consider d_1, which is already routed. Suppose we want to determine if moving d_2 to $(7, 4)$ is *implementable*. To actually move these two droplets to the desired cells, we need to activate (2,8) and (7,4). Four nodes $R(8)$, $C(2)$, $R(4)$ and $C(7)$ are created and *DIFF* edges are added between $R(8)$ and $C(2)$, and between $R(4)$ and $C(7)$. We can easily see that a two-coloring solution exists in the

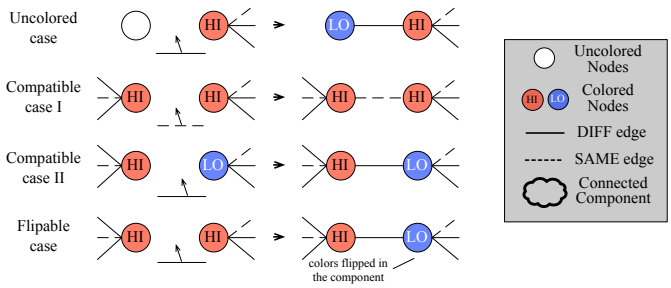

Fig. 8. Four cases of adding edge in incremental two-coloring.

constraint graph, and thus a valid voltage assignment exists to bring about the movements of the two droplets.

Fig. 7(b) illustrates the scenario that d_3 is being routed via some route while d_1 and d_2 are already routed. Specifically, suppose d_3 is routed to the place as shown in the figure, we need to decide the movement of next step of d_3. There are five possible choices to make, namely *up, down, left, right* and *stall*. Suppose now we want to determine whether moving right to cell $(4, 5)$ is *implementable*, we then perform the coloring steps as shown in Fig. 7(b). New nodes and edges are added based on the constraint graph in Fig. 7(a). The cells labeled with an $\times$ (cells (2,5), (2,4), (4,4) and (7,5)) are those that their row and column vertices exist in G_t, i.e., we need to assign a high or low voltage to them, but we want to make sure that they will not be activated. Therefore, *SAME* edges will be added between their row and column vertices. For this constraint graph, we can easily determine that no two-coloring exists, and thus there is no valid voltage assignment such that the three droplets can move simultaneously. Now it turns out that there is no valid assignment, the router will seek for another possible movement, such as moving up to $(3, 6)$. If all of the possible movements are not implementable, the router will drop this movement status and continue to search for other possible status. Another example that gives the detail of updating constraint graph after each propagation of net is given in Section IV-E after we introduce backtrack.

Note that this constraint graph seems to be similar to the interference graph with coalescing vertices in the *register allocation* problem. It is known that N-coloring on this type of graphs is NP-hard when $N \geqslant 3$, while the corresponding two-coloring problem is polynomial-time solvable. Adding the *SAME* edge constraint will not increase the problem difficulty, i.e., two-coloring of the proposed constraint graph is still polynomial-time solvable. Hence we can easily determine if the current movement of a droplet is feasible very efficiently by using the proposed method.

Finally, as mentioned in Section II-C, the guarding ring around a module cannot be activated during routing. This constraint can be simply added into the constraint graph as what we do for the droplets.

3) Incremental Coloring: In order to avoid constructing the graph from scratch for every electrode check, we implemented an *incremental* two-coloring in which the two-coloring results (with colors assigned to the vertices) are kept for later use. For each time step t, we keep a colored constraint graph G_t. These graphs will be updated and saved whenever a new

droplet is successfully routed. Specifically, every time a new net is routed, the corresponding new vertices and edges will be added into the constraint graph for each time step. The coloring solutions are preserved for later use. Given a time step t, we consider the routing of the next droplet d_j. We will reload the stored constraint graph G_t that contains the vertices and edges due to the movements of droplets $d_1, d_2, \ldots, d_{j-1}$ (assume that we process them in this order) at time t. When an edge $e = (u, v)$ is added due to this droplet d_j, we can check its *feasibility* as follows:

- If an edge exists between u and v already, we check the compatibility of e with the existing one. Report failure if the two edges are of different types.
- If no edge exist between u and v originally,
  - If either u or v has no color and its degree is 0 before adding the edge e, we can safely color it according to the type of e and the color of the other vertex.
  - If the type of e is compatible with the color of u and v, e.g., a *SAME* edge and both u and v are H, e can be safely added.
  - If the type of e is not compatible with the colors of u and v, we will try to *flip* the colors of all the vertices in u's (or v's) connected component. If the color of v (u) does not change after this flip operation, e can be safely added, otherwise the two-coloring is infeasible.

These four cases are summarized in Fig. 8.

4) Handling 3-pin net: Some nets may consist of more than one droplet. This kind of net is called 3-pin net, which models the operation of merging. In our method, each subnet is treated as a 2-pin net and routed to its sink separately. The droplet with a smaller Manhattan distance from the sink will be routed to the sink point first, and follows the other droplet. Note that they are only allowed to be merged when both are moving horizontally or vertically, instead of not one is moving horizontally and the other is moving vertically. More specifically, when the two droplets are in the same row or a same column and are separated by one cell, they will both be moved to the middle cell and merged. After the two droplets merge, they become one droplet that will then be routed to the sink point.

5) Waste Reservoir: Some droplets will be routed to a special location for disposal, i.e., *waste reservoir*. They will be routed to the waste reservoir and be removed from the biochip immediately it reaches there.

E. Backtracking Stage

After the current routing net reaches its sink point, a trace back is performed from its sink to its source to find out the actual path. Recall that to actually implement the routing of this droplet, we need to assign a voltage sequence to bring about the movements. The constraints that caused by this net, or equivalently, the corresponding vertices and edges, will be added into the constraint graph for each time step. Also, the coloring solution is added in an incremental manner. Note that if a droplet reaches its sink point before the time limit T. It will occupy the destination cell and act as a blockage for other droplets. Specifically, suppose a droplet reaches its sink at time t, it should stay at this sink point from time $t + 1$ to T. The fluidic and electrode constraint still apply. This subtle constraint must exist when processing the unrouted nets. Nevertheless, if this net's sink point is a waste reservoir, this droplet will be removed from the biochip at time $t + 1$ and thus no long be an obstacle to other droplets.

Here we show the backtrack stage by an example. Suppose the timing constraint $T = 5$, two droplets d_1 and d_2 are already routed. The constraint graphs for each time step are denoted as G_1, ..., G_5. The constraints to route d_1 and d_2 are already added in these graphs. We are routing droplet d_3, whose source and sink pin are $(0, 0)$ and $(2, 2)$, respectively. Assume that now we have successfully founded a path for d_3 at $t = 4$ during propagation stage, we then need to perform *backtrack* from $(2, 2)$. Since d_3 has already reached the sink, we can find the parent of $(2, 2)$ to know its previous location at $t = 3$ before reaching $(2, 2)$, and the parent of parent of $(2, 2)$ for its location at $t = 2$, and so on. When we are tracing back, we will add the nodes and edges that correspond to the constraints d_3 brings in into G_t, where $t \in [1..4]$. Meanwhile, G_t will be incrementally colored. Since the electrode constraint must be satisfied before d_3 reaches any position, these nodes and edges can be added safely and there must be a valid two-coloring solution in G_t. Note that d_3 reaches its sink at $t = 4$ while the timing limit is $T = 5$, which means d_3 will stay in its sink (2,2) for one more time step (suppose (2,2) is not a waste reservoir). Hence, when routing other unrouted droplets, they must be aware of this and should not violate the fluidic or electrode constraint with respect to d_3.

F. Rip-up and Re-route Nets

During the routing, for each net, the number of conflict it contributes to the current routing net will be recorded. When a valid path cannot be found for the current net, rip-up and re-route will be performed. The conflict counts will then serve as probabilities to determine which net to be ripped. The reason is that the larger conflict count a net has, the more possible that after this net is ripped, the current net can be successfully routed. More importantly, other nets with smaller conflict counts still have chance to be ripped. This randomness can effectively break the tie when some nets are ripping each other as a loop. Note that we start the conflict count from one in order to give every net a chance to be ripped.

G. Complexity

From Algorithm 1, it is clear that the propagation stage dominates the runtime complexity. At each time step t, there will be at most $O(WH)$ nodes be added into the queue. When operating on a node, a two-coloring of the constraint graph will be performed, which takes linear time as the size of the graph $O(WH)$. Hence, in the worst case traversing all these nodes within time limit T takes $O(TWH)$ time. There N nets to be routed. Therefore, the time and space complexity of the algorithm is $O(TNW^2H^2)$. Although this upper bound looks very large, the execution time is indeed short because the number of nodes to explore will be restricted

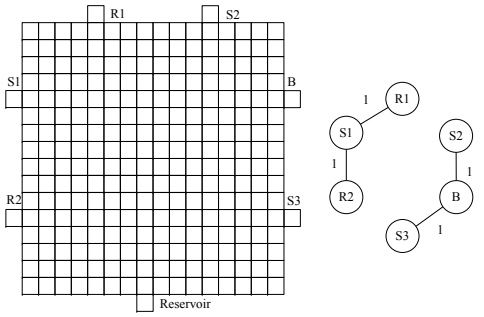

Fig. 9. Dispenser/reservoir distribution in *in-vitro*.

to a relatively small quantities due to the fluidic and electrode constraints. Furthermore, the two-coloring is performed in such a incremental manner that most of the cases are done in $O(1)$ time. The dominating factor is the timing limit T, whose size may not be polynomial-bounded by the input. However, T is reasonably small in the applications. Experimental results show that our router can find solutions in a time-efficient manner. Note that we do not include the running time of rip-up and re-route. Theoretically, the rip-up and re-route process will try all possible $n!$ permutations of the net ordering. However, in our implementation, we set a constant maximum count to limit the total number of trials. The rip-up and re-route time then becomes constant and we do not include it into the complexity.

V. Droplet-Routing-Aware Placement for Cross-Referencing Biochip

In this section, the proposed placement method will be discussed. Our method is droplet-routing-aware, and the properties of cross-referencing biochips are considered. Furthermore, the solutions obtained using our placement method will be evaluated using the cross-referencing biochip router proposed in the previous sections, which helps to test the qualities of the solutions. The proposed method consists of three stages: dispenser and reservoir location generation, solving the placement problem using ILP and pin assignment. Each of them will be further introduced in the following sections.

A. Problem Formulation

In architectural synthesis of DMFB, module placement is the step after task scheduling and resource binding. It can be viewed as a 3D-packing problem where the third dimension is time. The starting time of each operation corresponds to the z-value of the bottom plane of a specific module. Since the module size and time span have been determined during task scheduling and resource binding, the problem can be reduced to a series of 2D-packing problems at different time intervals. Specifically, whenever there are new modules that need to be placed into the layout region as time goes by, a new subproblem is created. The set of modules that need to be added are the objects we want to place. The existing on-going modules will act as blockages and the new modules shall not overlap with any of them. Hence, a set of consecutive subproblems will be defined from the given scheduling and binding result. After placement, all the droplets on the biochip must be routed to their destinations subject to some constraints. A formal description of the placement problem is given as follows:

- Input:
  - Scheduling and resource binding result
  - Chip specification, including time limit, chip size, optical detector number, reservoir/dispenser number
- Output:
  - Placement result, including module locations, reservoirs and dispensers and pin locations of each net
- Objective
  - Optimize the placement result such that it is easier for the proposed router to route.

B. Overview of Our Placement Method

Our placement method consists of three stages: dispenser and reservoir location generation, solving the placement problem using ILP and pin assignment. The first stage reads the input and decides the location of the dispensers and reservoirs. After these ports are determined, the placement problem is modeled as an ILP and solved by an ILP solver. Finally, after we obtained the module placement solustion from ILP, we need to generate pin locations as the input for the routing problem. The flow of the algorithm is summarized in Fig. 10.

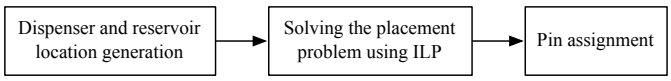

Fig. 10. Flowchart of the proposed placement method.

C. Dispenser and Reservoir Location Generation

This is a step to find the locations of the dispensers and reservoirs. The dispenser and reservoirs should be located on the boundary of the biochip. They are not fixed before placement. However, once decided, their location is fixed during the bioassay. Here, we do not put them into our Integer Linear Programming (ILP) formulation, but use a simple heuristic to place them on some computed positions. It is reasonable to distribute them using the proposed heuristic rather than giving them flexibility to locate arbitrarily on the boundary of the biochip, since some of them may cluster together and make the routing regions congested. More importantly, it can significantly reduce the solution space and the overheads by solving the ILP. The disadvantage is that the optimality of the solution may be hindered. But according to our experiment, the final result is mainly decided by the placement result. The algorithm is described as follows.

First of all, the waste reservoir is placed at the center of one side. A set of cells on the boundary of the biochip is then selected evenly according to the number of the reservoirs. Let there be N dispensers, we construct a graph with N vertices, where each vertex corresponds to a dispenser. For each operation in the bioassay, we check whether two dispensers

TABLE I
NOTATIONS USED IN ILP FORMULATION

M^i	Module i
M^i_x, M^i_y	Lower left coordinate of module M^i
$X(M^i)/Y(M^i)$	Width/Height of a mixing module i
W/H	Width/Height of the array.
$Center(M^i)$	Center point's coordinate of module M^i
L	A large constant
A_{ij}	Extended covered area bound by module/dispenser i and j

forms it. If it is true, the weight of the edge between the two corresponding vertices will be increment by one. If no edge between them, then an edge is inserted with weight equals to one. We define the weight of a vertex as the sum of the weight of all of its incident edges. After the graph is constructed, for each of the connected component, a vertex that has the largest weight is selected and inserted into a list. Its adjacent vertices are selected and inserted to head or tail of the list in turn. Finally, the elements in the list are arranged to the boundary clockwise (or counter-clockwise), starting from the waste reservoir position. This is based on the intuition that the larger weight a vertex has, the more central it should be placed in this component, such that the distance between it and the other dispensers are evenly distributed. An example is given in Fig. 9. It is from the *in-vitro* benchmark in Section VI.

D. Solving Placement Problem Using ILP

We formulate an ILP to solve the module placement problem while considering the properties of cross-referencing biochip. The module placement problem in electronic design is known to be NP-hard [30]. In order to solve it efficiently, we try to model the problem with a scalable size of variables and constraints. The core idea in the formulation is the definition of the objective function. In the ILP, the formulation is the sum of a series of *extended covered area* formed by the routes in each subproblem. The *extended covered area* of a rectangle is defined as the vertical and horizontal area span, as illustrated in Fig. 11(a). Since in cross-referencing DMFB, the droplet movement is controlled by applying different voltages to row and column. If the extended covered area of the bounding box of a route is minimized, the route is shorter. Furthermore, it helps to reduce the interference between routes. The notation used in our ILP formulation is shown in Table I. Note that the index is starting from 0.

1) Constraints:

a) Validity of modules: The modules should be inside the biochip. A further requirement is that the module including guarding ring should be at least one space away from the chip boundary. This constraint is needed in order not to block the route from the dispenser nor to the reservoir. Note that this guarding ring can be shared between different modules. For module i, the above requirement is represented as:

$$M^i_x \geqslant 2 \quad \wedge \quad M^i_x + X(M^i) \leqslant W - 2$$
$$M^i_y \geqslant 2 \quad \wedge \quad M^i_y + Y(M^i) \leqslant H - 2$$

b) Non-overlapping and separation of Modules: For modules that co-exist at some time, they must not overlap with each other. Furthermore, there should be a separation cell around each module. For a pair of module M^i and M^j which co-exist at the same time, we have the following constraints:

$$(M^j_x + X(M^j) < M^i_x - 1) \quad \vee \quad (M^i_x + X(M^i) < M^j_x - 1) \vee$$
$$(M^j_y + Y(M^j) < M^i_y - 1) \quad \vee \quad (M^i_y + Y(M^i) < M^j_y - 1)$$

Note that the '*or*' constraint cannot be directly written in linear programming and needs to be *linearized*. For this particular constraint, two binary variables are introduced. Let them be c_1 and c_2, the previous constraint is transformed to:

$$\begin{aligned} M^i_x - M^j_x - X(M^j) + L(c_1 + c_2) &> 1 \\ M^j_x - M^i_x - X(M^i) + L(c_1 + 1 - c_2) &> 1 \\ M^i_y - M^j_y - Y(M^j) + L(1 - c_1 + c_2) &> 1 \\ M^j_y - M^i_y - Y(M^i) + L(2 - c_1 - c_2) &> 1 \end{aligned}$$

where L is a large enough number (e.g., $W \times H$). It can be seen that among the four inequalities, only one of them will be left when the value of c_1 and c_2 are decided, others will be automatically satisfied due to the large value of L.

c) Droplet-Routing length constraint: The maximum length of droplet paths needs to be controlled, because large value of the path length leads to a long routing time, which may cause timing constraint violation. Furthermore, long routing length is prone to be blocked by other blocks on the way. Hence, it is necessary to have a constraint to limit the routing length to be smaller than the timing constraint. Nevertheless, since we are not computing the actual routing path during the placement phase, we will allow some degree of excess, i.e., relaxation of maximum routing length. For a routing path to be completed between two modules M^i and M^j, the relaxation of maximum routing length is determined by the module size of M^j. Without loss of generality, suppose M^i locates to the lower left of M^j, source pin and sink pin are generated around M^i and M^j respectively. In the worst case, the droplets have to departure from the lower left corner of M^i, and arrives at the upper right corner of M^j. Hence, the relaxation value is set to $X(M^j)+Y(M^j)+d$, where d is a fixed parameter that can be tuned to allow extra relaxation for a congested layout area (recall that the droplet may encounter blockages during routing). An illustration is given in Fig. 11(b).

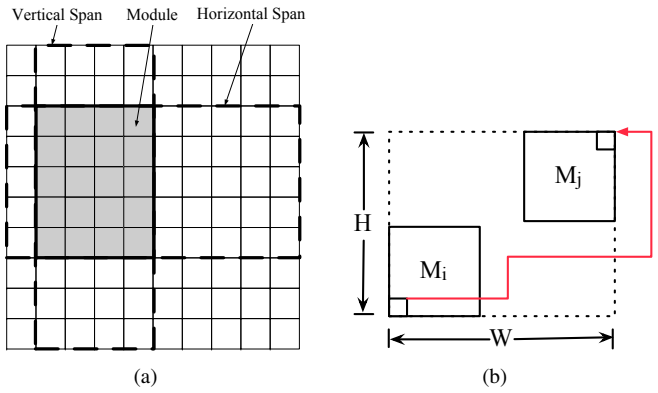

Fig. 11. (a) Illustration of extended covered area. (b) Illustration of droplet routing path, where W=$M^j_x - M^i_x + X(M^j)$, H=$M^j_y - M^i_y + Y(M^j)$. Note that there is detour. Hence, the length of the path is $W + H + len\_detour$, where len_detour is the length of the detour.

The constraint is modeled as follows:

$$M_x^j - M_x^i + M_y^j - M_y^i + X(M^j) + Y(M^j) + d \leqslant T$$

where T is the timing constraint of the biochip. This constraint help us to retain routability in the final placement result.

d) Optical detector resource constraint: Because optical detectors are limited and fixed in some specific locations on the chip, the modules that are assigned to the same optical detector must have the same coordinate on the chip. Let Dt denotes a set of modules that are bound to the same optical detector, we have:

$$(M_x^i, M_y^i) = (M_x^f, M_y^f),\ i \in Dt$$

where M^f is a module in Dt that first appear on the time line.

2) Objective: We use the bounding box as an estimation of the routes generated. Suppose that there is an operation, in which droplet i introduced by some module M^i is needed to be routed somewhere to form as input to M^j, we use the center points of both modules to form a bound box to model the route. Let $Center(M^i) = (x_i, y_i)$ and $Center(M^j) = (x_j, y_j)$, two pairs of variables, (x_{ll}, y_{ll}) and (x_{ur}, y_{ur}), are introduced to denote the bottom left corner and upper right corner of the bounding box formed by both center points.

$$\begin{array}{cccccccccc} x_{ll} & \leqslant & x_i, & x_{ll} & \leqslant & x_j, & x_{ur} & \geqslant & x_i, & x_{ur} & \geqslant & x_j \\ y_{ll} & \leqslant & y_i, & y_{ll} & \leqslant & y_j, & y_{ur} & \geqslant & y_i, & y_{ur} & \geqslant & y_j \end{array}$$

Then, we can compute the extended covered area bound by this route, denoted as A_{ij}:

$$A_{ij} = W(x_{ur} - x_{ll}) + H(y_{ur} - y_{ll})$$

The objective is to minimize the sum of all the extended covered area $\min \sum_k A_k$, where $A_k, k = 1, 2, ...$ is a set of all the extended covered area in the subproblems.

3) Problem Partition: Note that for some bioassays, there might be a large number of subproblems. When modeled as one ILP, the number of variables and constraints may be so huge that it is impossible to solve it efficiently. For example, there can be up to two thousands of variables and five thousands of constraints in the largest benchmarks that we use. Hence, it is necessary to control the problem size. The whole problem can be partitioned into manageable problem sub-sets if the original problem set is too large. An ILP can be set up and solved for problem sub-set, and the ILP result from the previous problem sub-sets should be input as constraints for the current problem sub-set. Different partitioning strategies can be adopted here. In our implementation, we adopt a simple partitioning scheme that regularly divides the original problem set into sub-sets of the same size. Each sub-set may contain seven to fifteen subproblems according to the chip size and the number of total subproblems in the benchmark. This strategy is simple yet working well according to the experimental result. For example, the benchmark *protein_2* that contains 78 subproblems can be partitioned into ten sets of consecutive subproblems $S_1 = \{s_i \mid i \in [1..10]\}$, $S_2 = \{s_j \mid j \in [11..20]\}$, ..., $S_6 = \{s_k \mid k \in [61..70]\}$ and $S_7 = \{s_l \mid l \in [71..78]\}$, where s_x for all $x \in [1..78]$ are the subproblems. While the original ILP formulation is too large to be solved, each of the subproblem sets can be solved in a time efficient manner.

TABLE II
COMPARISON BETWEEN PROGRESSIVE ILP AND CROSSROUTER

Circuit	#P[a]	Progressive ILP		CrossRouter		Improvement	
		Max/Avg cycle	CPU (s)	Max/Avg cycle	CPU (s)	Avg (%)	CPU (%)
*In-vitro*_1	11	24/13.09	2.55	20/12.09	0.92	8	64
*In-vitro*_2	15	22/11.00	2.53	19/10.73	1.21	2	52
Protein_1	64	26/16.15	15.36	20/15.52	7.76	4	49
Protein_2	78	26/10.23	6.70	20/9.86	2.22	4	69

[a]Number of subproblems in a benchmark.

E. Pin Assignment

After the exact locations of the modules are obtained by solving the above ILP formulation, the result is not complete enough for routing. According to the placement result from [25], we summarize the following rules:

- Mixing module is modeled as a 3-pin net;
- Dilute module is modeled as two 2-pin nets;
- Optical detection and storage are modeled as 2-pin nets.

The source pin and sink pin should locate around the bounding cells of the guarding ring of a module. Then, we have a set of possible locations for any specific pin. We will use a maze routing algorithm to help us to determine the best pin location that have a shorter routing distance. In particular, for a source pin and a sink pin, we have a set of possible source pin locations and a set of possible sink pin locations. We perform maze routing for each pair of the source and pin location, and select the pair that has the shortest routing distance as the final pins. Note that the pin locations should satisfy the fluidic constraint. For example, two source pins are not allowed to be adjacent. Otherwise, error may occur if two droplets comes out from the two pins in the same subproblem.

F. Complexity

The problem is modeled as an ILP and solved by lp_solver and the size of the ILP is dependent on the number of variables and constraints, which is a polynomial function of the chip size, number of subproblems and number of modules. The overall running time is exponential since ILP is NP-hard.

VI. EXPERIMENTAL EVALUATION

A. Overview of the Experiments

We use real-life bioassays as benchmarks. There are four sets of benchmarks, namely *in-vitro*, *in-vitro-2*, *protein* and *protein_2*, and there are 11, 15, 64 and 78 sub-problems in each benchmark, respectively. The *timing constraint* for every subproblem in each benchmark is 20 time units. To evaluate the proposed routing method, we will compare with the state-of-the-art work in paper [17]. Both of our and their programs are implemented in C++. Their program is executed on a 1.2GHz SUN Blade-2000 machine with 8GB memory, while our CrossRouter is executed on an Intel 1.6GHz machine[1] with 1.5GB memory. To evaluate our placement method, comparisons will be made between our work and the method

[1]We use the slowest machine that available to us in order to make fair comparisons.

TABLE III
COMPARISON BETWEEN [29] AND CROSSROUTER

Circuit	Size	# Cells used	
		HPDRA[a]	CrossRouter
*In-vitro*_1	16 × 16	258	246
*In-vitro*_2	14 × 14	246	254
Protein_1	21 × 21	1688	1668
Protein_2	13 × 13	963	936

[a]High Performance Droplet Routing Algorithm [29] for direct-addressing DMFBs.

proposed in paper [25]. Specifically, we will use our proposed CrossRouter to route the placement generated by [25] and the placements generated by our approach. Then, the solution qualities are compared. Our placement method is implemented in the C++ programming language, and the ILP part is solved using lp_solve 5.5 [31] and is run on a 2.4GHz Intel Core II Duo machine with 1.5GB memory. We limit the ILP solver to run for a given amount of time. The time limit is set to 30 minutes here, since from our empirical results, the quality of the solution is almost unchanged after 30 minutes.

B. Experimental Results

Table II gives the comparisons between progressive ILP [17] and CrossRouter. The "max cycle" in Table II stands for the time spent for routing the subproblem that takes the longest time to finish. And the "Avg cycle" stands for the average time to route a subproblem in a benchmark. The result shows that the routability of CrossRouter is better, since it can route all the subproblems within the timing constraint, while the progressive ILP approach in [17] has its maximum routing time exceeding the timing constraint. For instance, in the benchmark *in-vitro*_1, their router got a maximum finishing time of 24 cycles for some subproblems while ours are within the time limit of 20 cycles. Better results on average cycle time and CPU runtime are obtained, which demonstrates the good quality of our CrossRouter. Since the work in [17] does not optimize the number of cells used, we made another comparison with the router proposed in paper [29] (HPDRA), which is a droplet router for direct addressing biochips. Note that in direct addressing biochips, each cell can be activated independently, so there is no electrode interference and the droplet routing problem is much simpler. Table III shows that although the constraints are much harsher in the problem we are dealing with, our router can get better result in terms of the number of cells used among the four benchmarks, except for *In-vitro*_2. The reason is that in subproblem 2 of this benchmark, their router found an earlier merging point of a 3-pin net in comparison with ours.

Table IV summarizes the comparisons of our placement method and the approach in paper [25]. To compare both methods, we run the proposed router on the placement results generated from both methods, respectively. In the experiment, we define the *stalling steps* (SS) as the total number of stalling in the route that a droplet has taken. Stalling means that at a certain step, a droplet has to wait for the path to be cleared, either for waiting some other droplet to pass through, or by queueing outside the waste reservoir, etc. The major reason of stalling is due to the fluidic constraint, or more possibly, due to the electrode constraint for cross-referencing routing. For comparison, we run the router on the placement generated by [25] and on the placements generated by our approach. We can see from Table IV that by using the placement result generated by our proposed method, the max/avg cycles have been improved and the number of stalling steps is reduced. Moreover, it is shown that the number of cell used has been reduced by more than a half comparing with the routing result of the placement generated by [25]. According to the experiment result of max/avg cycle, we can see that the router can finish routing in a relatively shorter time, which indicates shorter route and less congestion.

VII. CONCLUSION

We presented a droplet-routing-aware placement method and a systematic routing method for cross-referencing digital microfluidics biochip. Electrode constraint is the most important issue in this type of DMFB. Our proposed router can handle the constraint elegantly and generates good quality solutions. To further improve the routing result, our placement method tries to utilize the property of cross-referencing DMFBs and generates placements that are more suitable for the router. The experiment result demonstrates the efficiency and effectiveness of the methods. By combining the effort of the placement and routing tool, the flexibility of cross-referencing DMFBs can be further exploited and the design and implementation of such chips can also be simplified.

REFERENCES

[1] M. Pollack, A. Shenderov, and R. Fair, "Electrowetting-based actuation of droplets for integrated microfluidics," *Lab on a Chip*, vol. 2, no. 2, pp. 96–101, 2002.

[2] E. Verpoorte and N. De Rooij, "Microfluidics meets MEMS," *Proceedings of the IEEE*, vol. 91, no. 6, pp. 930–953, 2003.

[3] T. Schulte, R. Bardell, and B. Weigl, "Microfluidic technologies in clinical diagnostics," *Clinica Chimica Acta*, vol. 321, no. 1-2, pp. 1–10, 2002.

[4] V. Srinivasan, V. Pamula, M. Pollack, and R. Fair, "Clinical diagnostics on human whole blood, plasma, serum, urine, saliva, sweat, and tears on a digital microfluidic platform," in *Proc. μTAS*, 2003, pp. 1287–1290.

[5] A. Guiseppi-Elie, S. Brahim, G. Slaughter, and K. Ward, "Design of a subcutaneous implantable biochip for monitoring of glucose and lactate," *IEEE Sensors Journal*, vol. 5, no. 3, pp. 345–355, 2005.

[6] R. Fair, A. Khlystov, T. Tailor, V. Ivanov, R. Evans, P. Griffin, V. Srinivasan, V. Pamula, M. Pollack, and J. Zhou, "Chemical and biological applications of digital-microfluidic devices," *IEEE Design & Test of Computers*, vol. 24, no. 1, pp. 10–24, 2007.

[7] E. Ottesen, J. Hong, S. Quake, and J. Leadbetter, "Microfluidic digital PCR enables multigene analysis of individual environmental bacteria," *Science*, vol. 314, no. 5804, pp. 1464–1467, 2006.

[8] Y. Zhao and S. Cho, "Microparticle sampling by electrowetting-actuated droplet sweeping," *Lab on a Chip*, vol. 6, no. 1, pp. 137–144, 2006.

[9] V. Srinivasan, V. Pamula, and R. Fair, "An integrated digital microfluidic lab-on-a-chip for clinical diagnostics on human physiological fluids," *Lab on a Chip*, vol. 4, no. 4, pp. 310–315, 2004.

[10] K. Chakrabarty, "Design Automation and Test Solutions for Digital Microfluidic Biochips," *IEEE Transactions on Circuits and Systems I: Regular Papers*, vol. 57, no. 1, pp. 4–17, 2010.

[11] Global In Vitro Diagnosis Market Analysis PRLog Free Pree Release. http://www.prlog.org/10080477-global-in-vitro-diagnostic-market-analysis.html.

[12] F. Su, W. Hwang, and K. Chakrabarty, "Droplet routing in the synthesis of digital microfluidic biochips," in *Proceedings of the Conference on Design, Automation and Test in Europe*, vol. 1, 2006, pp. 1–6.

TABLE IV
RUNNING CROSSROUTER UPON PLACEMENT [25] AND UPON OUR PLACEMENT

Name	#P*	Size	Routing result of [25]			Routing result of our placement			Improvement			
			Max/Avg cycle	SS †	Cell used	Max/Avg cycle	SS †	Cell used	Max	Avg	SS	Cell used
*in-vitro*_1	11	16 × 16	20/12.09	26	246	17/9.55	9	148	15%	21%	65%	40%
*In-vitro*_2	15	14 × 14	20/11.07	37	254	15/5.13	3	84	25%	54%	92%	67%
Protein_1	64	21 × 21	20/15.63	49	1668	20/11.66	33	925	0%	25%	33%	45%
Protein_2	78	13 × 13	20/9.86	42	936	19/8.14	31	662	5%	17%	26%	32%
								Average	11%	29%	54%	46%

*Number of subproblems

†Number of stalling steps

TABLE V
RUNNING [29] UPON PLACEMENT [25] AND UPON OUR PLACEMENT

Name	#P*	Size	Routing result of [25]		Routing result of our placement		Improvement		
			Max/Avg cycle	Cell used	Max/Avg cycle	Cell used	Max	Avg	Cell used
*in-vitro*_1	11	16 × 16	19/14.55	258	15/8.09	138	21%	44%	47%
*In-vitro*_2	15	14 × 14	20/11.87	246	18/6.07	115	10%	49%	53%
Protein_1	64	21 × 21	20/16.59	1688	20/10.53	983	0%	34%	42%
Protein_2	78	13 × 13	20/11.79	963	20/10.3	845	0%	13%	12%
						Average	8%	35%	38%

*Number of subproblems

[13] J. Ding, K. Chakrabarty, and R. Fair, "Scheduling of Microfluidic Operations for Reconfigurable Two-Dimensional Electrowetting Arrays," *IEEE Transactions on Computer Aided Design of Integrated Circuits and Systems*, vol. 20, no. 12, pp. 1463–1468, 2001.

[14] F. Su and K. Chakrabarty, "Architectural-level synthesis of digital microfluidics-based biochips," in *IEEE/ACM International Conference on Computer Aided Design*, 2004, pp. 223–228.

[15] T. Xu and K. Chakrabarty, "Droplet-trace-based array partitioning and a pin assignment algorithm for the automated design of digital microfluidic biochips," in *Proceedings of the 4th International Conference Hardware/Software Codesign and System Synthesis*, 2006, pp. 112–117.

[16] T. Xu and K. Chakrabarty, "Broadcast electrode-addressing for pin-constrained multi-functional digital microfluidic biochips," in *Proc. of the 45th Annual Design Automation Conference*, 2008, pp. 173–178.

[17] P. Yuh, S. Sapatnekar, C. Yang, and Y. Chang, "A progressive-ILP based routing algorithm for cross-referencing biochips," in *Proceedings of the 45th annual Design Automation Conference*, 2008, pp. 284–289.

[18] M. Sarrafzadeh and C. Wong, *An introduction to VLSI physical design*. McGraw-Hill Higher Education, 1996.

[19] F. Su and K. Chakrabarty, "Design of fault-tolerant and dynamically-reconfigurable microfluidic biochips," in *Proceedings of the Conference on Design, Automation and Test in Europe*, 2005, pp. 1202–1207.

[20] F. Su and K. Chakrabarty, "Unified high-level synthesis and module placement for defect-tolerant microfluidic biochips," in *Proceedings of the 42nd Annual Conference on Design Automation*, 2005, pp. 825–830.

[21] T. Xu and K. Chakrabarty, "Integrated droplet routing in the synthesis of microfluidic biochips," in *Proceedings of the 44th Annual Conference on Design Automation*, 2007, pp. 948–953.

[22] K. Bazargan, R. Kastner, and M. Sarrafzadeh, "Fast template placement for reconfigurable computing systems," *IEEE Design & Test of Computers*, vol. 17, no. 1, pp. 68–83, 2000.

[23] P. Yuh, C. Yang, Y. Chang, and H. Chen, "Temporal floorplanning using 3D-subTCG," in *Proceedings of the 2004 Asia and South Pacific Design Automation Conference*, 2004, pp. 725–730.

[24] P. Yuh, C. Yang, and Y. Chang, "Temporal floorplanning using the T-tree formulation," in *Proceedings of the IEEE/ACM International Conference on Computer Aided Design*, 2004, pp. 300–305.

[25] P. Yuh, C. Yang, and Y. Chang, "Placement of defect-tolerant digital microfluidic biochips using the T-tree formulation," *ACM Journal on Emerging Technologies in Computing Systems*, vol. 3, no. 3, Article 13, 2007.

[26] E. Griffith, S. Akella, and M. Goldberg, "Performance characterization of a reconfigurable planar-array digital microfluidic system," *IEEE Transactions on Computer Aided Design of Integrated Circuits and Systems*, vol. 25, no. 2, pp. 345–357, 2006.

[27] E. Griffith and S. Akella, "Coordinating multiple droplets in planar array digital microfluidic systems," *The International Journal of Robotics Research*, vol. 24, no. 11, pp. 933–949, 2005.

[28] T. Xu and K. Chakrabarty, "A cross-referencing-based droplet manipulation method for high-throughput and pin-constrained digital microfluidic arrays," in *Design, Automation & Test in Europe Conference & Exhibition*, 2007, pp. 1–6.

[29] M. Cho and D. Pan, "A high-performance droplet router for digital microfluidic biochips," in *Proceedings of the 2008 International Symposium on Physical Design*, 2008, pp. 200–206.

[30] M. Garey and D. Johnson, *Computers and intractability: A Guide to the Theory of Computers and Intractability*. WH Freeman and Company, San Francisco, Calif, 1979.

[31] http://lpsolve.sourceforge.net.

Zigang Xiao received the B.S. degree in Computer Science from Sun Yat-sen (Zhongshan) University, Guangzhou, China, in 2008, and the M.Phil. degree in Computer Science from the Chinese University of Hong Kong, Shatin, Hong Kong, China, in 2010. He is currently working toward the Ph.D. degree at the Department of Electrical and Computer Engineering, University of Illinois at Urbana-Champaign, Champaign, United States. His research interests include physical design of very large scale integration circuits and algorithm design.

Evangeline F. Y. Young Evangeline Young received her B.Sc. degree and M.Phil. degree in Computer Science from The Chinese University of Hong Kong (CUHK). She received her Ph.D. degree from The University of Texas at Austin in 1999. Currently, she is an associate professor in the Department of Computer Science and Engineering in CUHK. Her research interests include algorithms and CAD of VLSI circuits. She is now working actively on floorplanning, placement, routing and algorithmic designs. Dr. Young has served on the technical program committees of several major conferences including ICCAD, ASP-DAC, ISPD and GLSVLSI, and also served on the editorial board of IEEE TCAD.